

## Experimental and Theoretical Analysis of Vicinal and Long-Range Proton–Proton Coupling Constants for Anthracene Derivatives

Ernesto Sánchez-Mendoza,<sup>†</sup> Jesús Hernández-Trujillo,<sup>‡</sup> and Federico del Río-Portilla<sup>\*,†</sup>

Departamento de Bioquímica, Instituto de Química, and Departamento de Física y Química Teórica, Facultad de Química, Universidad Nacional Autónoma de México, Circuito Exterior s/n, Ciudad Universitaria, México D. F. 04510, México

Received: May 10, 2007; In Final Form: June 27, 2007

We studied vicinal and long-range coupling constants for 9-anthracene derivatives, e.g., Br, CN, CHO, NO<sub>2</sub>, CH<sub>2</sub>Cl, CH<sub>2</sub>OH, and OCH<sub>3</sub>. We performed the accurate measurements using modified *J* doubling in the frequency domain, even for the smallest couplings immersed within the line width. Density functional theory allowed us to reproduce and exhaustively analyze the physical contributions to the values of these spectroscopic parameters. The theory of atoms in molecules defines a delocalization index that correlates linearly with vicinal and long-range coupling constants when they are grouped in terms of the number of bonds between the coupled nuclei. An exception to this behavior is obtained for <sup>4</sup>*J*<sub>H4,H10</sub> values, which have a negative Fermi contact and the largest delocalization index for each molecule. This observation can be explained by a characteristic “gable roof” arrangement formed by the five nuclei involved in the coupling.

### Introduction

The availability of highly precise experimental procedures for the accurate determination of long-range coupling constants and the existence of theoretical methods to predict their values and contributions have oriented our efforts toward an exhaustive analysis of these parameters for 9-anthracene derivatives. In this contribution, we studied the vicinal and long-range coupling constants of this type of molecules with the best accurate experimental determinations, in order to compare with modern theoretical methods and also to provide a physical interpretation of these parameters.

NMR spectroscopy is an indispensable technique for the determination of molecular structure. The nuclear shielding constants and scalar spin–spin coupling constants provide invaluable information of the electronic structure. The vicinal and long-range proton–proton coupling constants comprise a powerful tool for the structure elucidation and conformational analyses of molecules in solution. The size of the coupling constant depends on both the number of bonds that separate the interacting nuclei and the electronic configuration of the molecule. Normally, the measurement of experimental coupling constants in aromatic systems has been carried out by estimation or by simulation using higher order multiplets, although such approaches increase the uncertainty in the comparison between the experimental and theoretical results. The vertiginous development of new methods to predict theoretical coupling constants requires the most accurate experimental determinations, in which several factors interfere, e.g., strongly coupled systems, couplings immersed in the signals, and overlapped and/or complex multiplets. Problems of overlapping and strongly coupled systems can be partially solved by increasing the magnetic field. Nowadays, a large number of experimental techniques capable

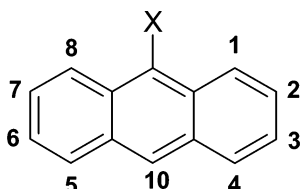
of measuring coupling constants immersed in both the signal and in complex multiplets have been developed.<sup>1</sup> One of the most sensitive methods is the modified *J* doubling in the frequency domain.<sup>2</sup> This method uses a set of delta functions (... +1, -1, +1, +1, -1, +1, ...) for in-phase multiplets. These delta functions are defined in the given reference and must not be confused with the chemical shift symbol or the delocalization index defined below. The convolution process, together with the coupling found for it, generates a simplified multiplet that preserves the integral and the position of the original one. If the number of delta functions tends to infinity, the whole operation behaves as a formal deconvolution of the signal, which is a linear process. Modified *J* doubling allowed us to measure very small coupling constants (~0.3 Hz) even if they are immersed in complex multiples and within the line width at the same time.<sup>2–4</sup> This method has the advantage of accurately measuring the magnitude of coupling constants while deconvolving the signals at the same time for nonoverlapped first-order multiplets. At this moment, this is the only method available for the measurement of several small coupling constants immersed in complex multiplets and within the line width.

During the last decades, quantum chemistry has focused on the calculation and spectral prediction of these parameters. Most of the theoretical descriptions of spin–spin coupling constants follow the Ramsey and Purcell interpretation<sup>5</sup> and Ramsey formulation.<sup>6</sup> All coupling constants in this work are calculated by adding four different terms: (1) diamagnetic spin–orbit (DSO) and (2) the paramagnetic spin–orbit (PSO), which represent the interactions of the magnetic field of the nuclei mediated by the electron orbital motion; (3) the Fermi contact (FC), which is also a response property reflecting the interaction between the electron spin magnetic moment close to the nucleus and the magnetic field at the nucleus; and (4) the spin-dipole (SD), which describes the interactions between the nuclear magnetic moments as mediated by the electronic spin angular

\* To whom correspondence should be addressed. Tel. (+52) 55 56224613. Fax: (+52) 55 562162203. E-mail: jfrp@servidor.unam.mx.

<sup>†</sup> Departamento de Bioquímica.

<sup>‡</sup> Departamento de Física y Química Teórica.



9-substituent	H1	H2	H3	H4	H10
Br	8.47	7.55	7.46	7.95	8.39
CN	8.42	7.71	7.58	8.07	8.66
CHO	8.97	7.67	7.54	8.05	8.67
NO <sub>2</sub>	8.03	7.62	7.53	7.92	8.57
CH <sub>2</sub> OH	8.42	7.57	7.49	8.03	8.47
CH <sub>2</sub> Cl	8.33	8.04	7.62	7.52	8.49
OCH <sub>3</sub>	8.29	~7.46	~7.46	7.98	8.20

**Figure 1.** 9-Substituted anthracene derivatives used for this study ( $X = \text{Br}, \text{CN}, \text{NO}_2, \text{CH}_2\text{Cl}, \text{CH}_2\text{OH}, \text{CHO}, \text{OCH}_3$ ) and their experimental chemical shift in  $\text{CDCl}_3$  referenced with respect to TMS.

momenta. All mechanisms may be important and none can be a priori neglected.<sup>7–12</sup>

Since Karplus<sup>13–15</sup> described the relationships between three-bond coupling constants,  ${}^3J$ , and the H–C–C–H dihedral angle in ethane, many papers have been published where structure or conformation of complex systems are inferred from this property.<sup>16,17</sup> In addition,  ${}^4J$  for H–C–C–C–H fragments with a planar W conformation are the most used long-range coupling constants for structural and conformational assignment.<sup>18,19</sup> However, Karplus relation is not used to describe vicinal coupling constants for unsaturated compounds with  $\pi$  electrons.<sup>20</sup> In the case of aromatic and double bonded molecules, the coupling can be transmitted through both the  $\sigma$  framework and  $\pi$  system, which is assumed to be the main contribution to long-range couplings in this type of compounds.<sup>20,21</sup>

Coupling constants between vicinal H atoms have been interpreted in terms of electron delocalization defined from the integration of the Fermi-hole density over the basins of the H

atoms defined by the quantum theory of atoms in molecules.<sup>22</sup> Within the Hartree–Fock or KS approximations, a delocalization index between the atoms H and H' can be defined as<sup>23</sup>

$$\delta(\text{H,H}') = 4 \sum_{ij} S_{ij}(\text{H}) S_{ij}(\text{H}') \quad (1)$$

In this expression, the sums run over all of the molecular orbitals; and  $S_{ij}(\text{H})$  and  $S_{ij}(\text{H}')$  are the overlap integrals of molecular orbitals  $i$  and  $j$  over the basins of atoms H and H', respectively.  $\delta(\text{H,H}')$  must not be confused with the chemical shift symbol. Accordingly,  $\delta(\text{H,H}')$  provides a measure of the number of electrons shared between the atoms H and H'. For example, the values of  $\delta(\text{H,H}')$  as a function of the H–C–C–H dihedral angle in ethane display the same behavior as that found by Karplus for the corresponding coupling constants.<sup>24</sup> It has also been reported<sup>25</sup> that for a number of organic molecules, including polybenzenoid hydrocarbons, the Fermi contact produces a dominant contribution to the  ${}^3J_{\text{HH}'}$  values; hence, this property mainly results from the coupling of nuclear spins mediated by the electronic spins with this dominant term of the s-type orbitals at the nuclear positions. In addition, satisfactory empirical correlations between  ${}^3J_{\text{HH}'}$  and  $\delta(\text{H,H}')$  have been obtained, thus supporting the conclusion that proton–proton vicinal coupling constants are a consequence of electron delocalization and exemplify how the Fermi exchange density contains information related to nonbonded atoms.<sup>25,26</sup>

Anthracene is a polybenzenoid compound that has been used in several theoretical studies because of its symmetry, aromaticity, and rigid geometry.<sup>27–29</sup> We present, in this work, a complete study of experimental and theoretical vicinal and long-range coupling constants for 9-anthracene derivatives that present weak coupling constants and none or few overlapped signals. Multiplets with these restrictions can be used to determine the most possible accurate experimental results. We

**TABLE 1: Experimental and Theoretical Values of Vicinal and Long-Range Coupling Constants of 9-Substituted Anthracenes and Delocalization Indexes<sup>a</sup>**

		Br			CN			CH <sub>2</sub> Cl			CH <sub>2</sub> OH			CHO			NO <sub>2</sub>			OCH <sub>3</sub>		
		$J_{\text{cal}}$	$J_{\text{exp}}$	$\delta(\text{H,H}')$	$J_{\text{cal}}$	$J_{\text{exp}}$	$\delta(\text{H,H}')$	$J_{\text{cal}}$	$J_{\text{exp}}$	$\delta(\text{H,H}')$	$J_{\text{cal}}$	$J_{\text{exp}}$	$\delta(\text{H,H}')$	$J_{\text{cal}}$	$J_{\text{exp}}$	$\delta(\text{H,H}')$	$J_{\text{cal}}$	$J_{\text{exp}}$	$\delta(\text{H,H}')$	$J_{\text{cal}}$	$J_{\text{exp}}$	$\delta(\text{H,H}')$
${}^3J_{\text{H1-H2}}$	1	8.44	8.88	646	7.99	8.70	630	8.07	8.89	654	8.02	8.89	664	8.04	9.01	576	8.70	8.86	662	7.41	8.26	621
	2	9.30			8.84			8.88			8.84			8.89			9.53			8.21		
	3	6.63			6.22			6.45			6.40			6.24			6.74			5.86		
${}^3J_{\text{H2-H3}}$	1	5.88	6.49	526	5.92	6.58	528	5.75	6.45	518	5.70	6.43	519	5.65	6.53	509	5.64	6.55	517	5.63		523
	2	6.54			6.57			6.41			6.35			6.30			6.27			6.25		
	3	4.25			4.27			4.18			4.15			4.13			3.98			4.00		
${}^3J_{\text{H3-H4}}$	1	7.65	8.45	643	7.64	8.50	639	7.48	8.46	626	7.48	8.44	631	7.25	8.45	605	7.86	8.52	664	7.41	7.94	638
	2	8.45			8.45			8.29			8.29			8.06			8.65			8.21		
	3	6.06			6.04			5.96			5.97			5.77			6.11			5.86		
${}^4J_{\text{H1-H3}}$	1	0.71	1.11	150	0.61	1.10	154	0.58	1.00	156	0.60	1.10	159	0.59	1.05	132	0.53	1.07	137	0.64		163
	2	0.29			0.16			0.16			0.16			0.14			0.10			0.18		
	3	-0.78			-0.95			-0.90			-0.90			-1.01			-0.91			-0.94		
${}^4J_{\text{H2-H4}}$	1	0.74	1.26	177	0.69	1.22	173	0.79	1.32	181	0.79	1.36	183	0.88	1.38	185	0.71	1.22	174	0.64		175
	2	0.28			0.23			0.34			0.34			0.41			0.27			0.18		
	3	-0.82			-0.90			-0.81			-0.80			-0.80			-0.81			-0.94		
${}^4J_{\text{H4-H10}}$	1	-0.36	0.60	913	-0.41	0.61	865	-0.41	0.61	916	-0.41	0.61	936	-0.44	0.60	948	-0.28	0.60	919	-0.41	0.59	844
	2	0.09			0.04			0.03			0.02			-0.01			0.21			0.03		
	3	0.74			0.66			0.66			0.65			0.53			0.96			0.59		
${}^5J_{\text{H1-H4}}$	1	0.87	0.76	34.0	0.82	0.82	35.3	0.85	0.81	35.3	0.83	0.79	36.5	0.83	0.81	28.7	0.70	0.82	31.7	0.85		35.6
	2	0.68			0.61			0.66			0.64			0.63			0.47			0.64		
	3	0.34			0.26			0.36			0.35			0.37			0.06			0.32		
${}^5J_{\text{H1-H10}}$	1	0.85	0.95	53.9	0.82	0.98	56.3	0.88	1.1	57.9	0.85	0.94	59.0	0.84	0.94	51.9	0.67	0.98	52.4	0.80	0.98	56.3
	2	0.77			0.73			0.80			0.77			0.75			0.55			0.71		
	3	0.35			0.33			0.43			0.43			0.50			0.04			0.37		
${}^5J_{\text{H3-H10}}$	1	0.44	0.38	15.1	0.41	0.38	14.4	0.43	0.39	14.8	0.43	0.38	15.1	0.43	0.36	14.3	0.35	0.38	16.2	0.41	0.36	14.4
	2	0.40			0.37			0.40			0.39			0.40			0.29			0.38		
	3	0.20			0.19			0.24			0.24			0.32			0.06			0.19		

<sup>a</sup> Experimental values ( $J_{\text{exp}}$ ) are the averages between the measurements obtained by modified  $J$  doubling in the multiplets involved. Theoretical values ( $J_{\text{cal}}$ ) were obtained at three levels of theory: (1) B3LYP/6-311+G(2d,p), (2) B3LYP/6-31G\*\*, and (3) B3LYP/STO-3G. Delocalization indices  $\delta(\text{H,H}') \times 10^5$  were calculated only using B3LYP/6-311+G(2d,p), which shows the better results.

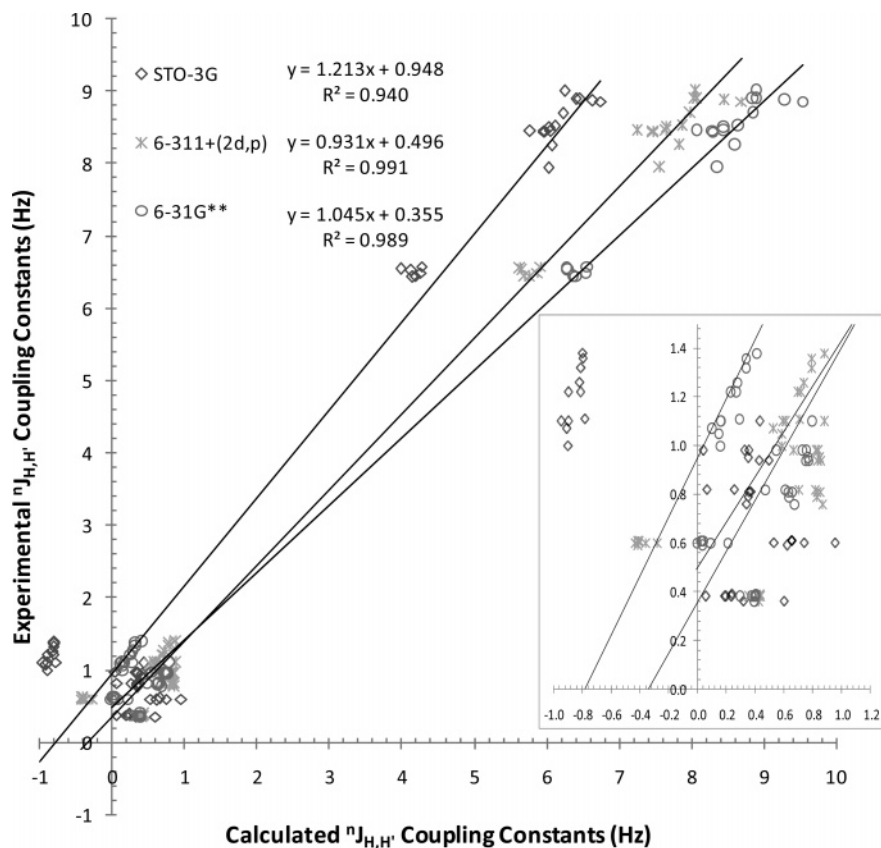


**Figure 2.** Correlation between experimental and theoretical coupling constants for all compounds shown in Figure 1 and for B3LYP/6-311+G-(2d,p), B3LYP/6-31G\*\*, and B3LYP/STO-3G levels of theory. (Inset) An expansion of the region at small coupling constants. All  ${}^3J_{H,H'}$  were plotted with their absolute experimental values vs their theoretical ones. This plot shows that the coupling constant can be grouped accordingly by type and does not depend on the substituent, except for  ${}^3J_{H1,H2}$ .

discarded several derived compounds that do not comply with these restrictions. The experimental analysis comprises the determination of the magnitude and most of the coupling constant signs. On the other hand, the theoretical study includes the calculation of the four contributions at several levels of theory and their relation with the experimental values. In addition, we tested the ability of the delocalization index to explain the trends of the Fermi contact term in the case of four- and five-bond distance H,H' couplings. In this manner, a consistent picture of experimental coupling constants of small magnitude, their theoretically obtained contributions, and the relationship with the electronic structure of the interacting atoms is achieved, providing a physical meaning for long-range coupling constants in 9-substituted anthracenes. It is known that vicinal coupling constants do not vary significantly with the solvent,<sup>30</sup> and Katritzky<sup>31</sup> has reported that theoretical calculations underestimate vicinal and long-range coupling constants; considering these facts, we did not consider the solvent effects in this work.

## Results and Discussion

The 9-anthracene derivatives displayed in Figure 1 were selected for the study on the basis of their availability and stability. We only worked with typical first-order and nonoverlapped multiplets. All signals were extracted and their coupling constants determined by the modified  $J$  doubling method. The reported values are the average between the determinations measured in both multiplets. In the worst cases, the accuracy is better than  $\pm 0.04$  Hz. No experimental results have been reported before at this level of accuracy for anthracene derivatives. In total, we could measure 20 vicinal and 39 long-range

coupling constants and determine 39 signs, which are reported in Table 1.  ${}^3J_{H2,H3}$ ,  ${}^4J_{H1,H3}$ ,  ${}^4J_{H2,H4}$ , and  ${}^5J_{H1,H4}$  of 9-methoxyanthracene were not determined because of the lack of first-order signals. Coupling constant signs were obtained by the double resonance method.<sup>32</sup> Signs of  ${}^4J_{H1,H3}$  and  ${}^4J_{H2,H4}$  are positive for all systems, as described by Günther;<sup>33</sup> however, we were unable to determine those of  ${}^4J_{H4,H10}$ , because no significant modification is observed on the H10 multiplet (an apparent singlet) when the appropriate region of the H4 signal is irradiated. Theoretical calculations give uncertain signs for all  ${}^4J_{H4,H10}$  values; they depend on the level of theory used.

The coupling constants were predicted within the density functional theory (DFT) approach with the gauge-including atomic orbital (GIAO) method including the four contributing terms and the B3LYP density exchange-correlation potential with *Gaussian 03*.<sup>34</sup> The B3LYP density functional provides accurate coupling constant values in many systems.<sup>35</sup> Our discussion will focus on the STO, 6-31G\*\*, and 6-311+G(2d,p) basis sets. The overlap integrals over the topological atoms in the molecules were computed with the program *AIMALL97*<sup>36</sup> and the delocalization indexes were obtained according to eq 1. We analyzed our results accordingly with the number of bonds involved in the coupling and discuss the contribution from the theoretical calculation and correlate the Fermi contact term with the delocalization index.

**Vicinal Coupling Constants ( ${}^3J_{H,H}$ ).** The experimental values for  ${}^3J_{H1,H2}$ ,  ${}^3J_{H2,H3}$ , and  ${}^3J_{H3,H4}$  of all 9-anthracene derivatives lie within the ranges 8.4–9.01, 6.43–6.58, and 8.44–8.48 Hz, respectively. An excellent correlation with the experimental values is obtained using the B3LYP/6-31G\*\* level of theory. For example, for 9-bromineanthracene  ${}^3J_{H3,H4}$  has the same value

(8.45 Hz), and seven theoretical calculations have less than 1% error. We observed that whereas B3LYP/STO-3G underestimates all of the vicinal coupling constants, B3LYP/6-311+G(2d,p) overestimates them. In agreement with the results shown in Table 1,  ${}^3J_{\text{H}_1\text{H}_2}$  is the most sensitive constant to the electronic modifications caused by the substituent. The comparison between experimental and theoretical coupling constants is plotted in Figure 2. In keeping with previous reports<sup>25</sup> on  ${}^3J_{\text{HH}'}$  of polybenzenoid hydrocarbons, these coupling constants are dominated by the Fermi contact term, the sum of SD, PSO, and DSO being close to zero; see the Supporting Information.

**Long-Range Coupling Constants ( ${}^4J_{\text{H,H}}$ ,  ${}^5J_{\text{H,H}}$ ).** Whereas a calculation of the Fermi contact term can predict  ${}^3J_{\text{HH}'}$  values within an error less than 2%, the prediction of long-range coupling constants requires the four terms; all mechanisms are important and none can be neglected. The experimental coupling constants  ${}^4J_{\text{H}_1\text{H}_3}$ ,  ${}^4J_{\text{H}_2\text{H}_4}$ , and  ${}^4J_{\text{H}_4\text{H}_{10}}$  are within the range 1.0–1.1, 1.22–1.38, and 0.58–0.60 Hz, respectively. Unexpectedly, the absolute values of four-bond coupling constants are better reproduced with the B3LYP/STO-3G level of theory; although this could be a fortuitous result. Six coupling constants were obtained with an error of less than 10% with respect to the experiment. We obtained the best result for  ${}^4J_{\text{H}_4\text{H}_{10}}$  (absolute values: experimental, 0.61 Hz; theoretical, 0.65 Hz) for 9-(methylchloro)anthracene. Thirteen four-bond coupling constants have an error lower than 30% with respect to the experimental value; these results could be considered a good approximation for this kind of coupling.<sup>31,37</sup> The analysis of the contributions for  ${}^4J_{\text{H,H}'}$  through different basis sets indicates that the PSO term is substantially modified with the STO-3G basis set; see Table 2 for 9-cyanoanthracene. This behavior is observed for all systems under study. The modification of the PSO value may be the term responsible for the magnitude of the four-bond coupling constants. Experimental signals for  ${}^4J_{\text{H}_4\text{H}_{10}}$  were impossible to measure.

The experimental coupling constants  ${}^5J_{\text{H}_1\text{H}_4}$ ,  ${}^5J_{\text{H}_1\text{H}_{10}}$ , and  ${}^5J_{\text{H}_3\text{H}_{10}}$  are in the range 0.79–0.82, 0.94–1.10, 0.36–0.39 Hz, respectively. Five-bond distance coupling constant values are dominated by the Fermi contact; although, the calculated value accuracy depends on all contributions. In general, the experimental measurements are better reproduced using the B3LYP/6-311+G(2d,p) level of theory. There is an excellent agreement with the experimental result for  ${}^5J_{\text{H}_1\text{H}_4}$  of 9-cyanoanthracene; both values give 0.82 Hz (see Table 2). The analysis of all long-range coupling constants indicates that the magnitude of the coupling does not undergo substantial modification when the substituent in the anthracene derivatives is changed.

Our results show that each type of coupling constant is better reproduced with a specific level of theory. However, the 6-311+G(2d,p) basis set reproduces all experimental values with a good approximation. We used the B3LYP/6-311+G(2d,p) level of theory for subsequent studies.

**Coupling Constants and Electron Delocalization.** For the following discussion, we used the results corresponding to the B3LYP/6-311+G(2d,p) level of theory. We analyze the relationship between experimental coupling constants and the Fermi contact term with the delocalization indices defined in eq 1, according with the number of bonds involved (Table 1). Generally speaking, there is a linear correlation between all  ${}^3J_{\text{H,H}}$  and the delocalization indices. The same result can be observed for  ${}^4J_{\text{H,H}}$  and  ${}^5J_{\text{H,H}}$  except for  ${}^4J_{\text{H}_4\text{H}_{10}}$ . All couplings should be grouped for their analysis. In the case of three-bond couplings, the value of the delocalization index  $\delta(\text{H}_2,\text{H}_3)$  is smaller than

**TABLE 2: Four Coupling Constant Terms for 9-Cyanoanthracene<sup>a</sup>**

	CN	FC	SD	PSO	DSO	$J_{\text{cal}}$	$J_{\text{exp}}$
${}^3J_{\text{H}_1\text{H}_2}$	1	8.186	0.022	−0.047	−0.167	7.99	8.70
	2	9.002	0.028	−0.013	−0.177	8.84	
	3	6.687	0.026	−0.35	−0.138	6.22	
${}^3J_{\text{H}_2\text{H}_3}$	1	5.968	0.089	0.184	−0.321	5.92	6.58
	2	6.591	0.091	0.217	−0.329	6.57	
	3	4.648	0.076	−0.167	−0.292	4.27	
${}^3J_{\text{H}_3\text{H}_4}$	1	7.877	0.013	0.085	−0.332	7.64	8.50
	2	8.686	0.021	0.080	−0.341	8.45	
	3	6.637	0.016	−0.312	−0.305	6.04	
${}^4J_{\text{H}_1\text{H}_3}$	1	0.830	0.036	1.437	−1.694	0.61	1.10
	2	0.726	0.035	1.098	−1.701	0.16	
	3	0.411	0.087	0.229	−1.675	−0.95	
${}^4J_{\text{H}_2\text{H}_4}$	1	0.923	0.040	1.491	−1.760	0.69	1.22
	2	0.825	0.039	1.135	−1.767	0.23	
	3	0.508	0.091	0.244	−1.742	−0.90	
${}^4J_{\text{H}_4\text{H}_{10}}$	1	−0.669	0.006	−1.608	1.863	−0.41	0.61
	2	−0.642	0.007	−1.192	1.868	0.04	
	3	−0.659	−0.097	−0.451	1.864	0.66	
${}^5J_{\text{H}_1\text{H}_4}$	1	0.902	0.172	1.449	−1.705	0.82	0.82
	2	1.040	0.173	1.110	−1.711	0.61	
	3	1.376	0.281	0.287	−1.688	0.26	
${}^5J_{\text{H}_1\text{H}_{10}}$	1	0.979	0.039	1.119	−1.318	0.82	0.98
	2	1.155	0.039	0.859	−1.322	0.73	
	3	1.299	0.114	0.221	−1.306	0.33	
${}^5J_{\text{H}_3\text{H}_{10}}$	1	0.509	−0.033	0.640	−0.703	0.41	0.38
	2	0.607	−0.034	0.507	−0.706	0.37	
	3	0.820	−0.064	0.126	−0.697	0.19	

<sup>a</sup> Experimental values ( $J_{\text{exp}}$ ) are the averages between the measurements obtained by modified  $J$  doubling in the multiplets involved. Theoretical values ( $J_{\text{cal}}$ ) were obtained at three levels of theory: (1) B3LYP/6-311+G(2d,p), (2) B3LYP/6-31G\*\*, and (3) B3LYP/STO-3G. FC, Fermi contact; SD, spin-dipole; PSO, paramagnetic spin-dipole; and DSO, diamagnetic spin-dipole.

$\delta(\text{H}_1,\text{H}_2)$  and  $\delta(\text{H}_3,\text{H}_4)$ . This behavior is also observed for the Fermi contact term, which follows the same trend as the corresponding experimental coupling constants.

All three different types of  ${}^5J_{\text{H,H}}$  follow a linear behavior with the delocalization index, despite the small values of the latter, as shown in Figure 3a, following the same tendencies as that of the three-bond couplings. In this figure, the presence of three groups related to the three different types of five-bond couplings measured is clear. We observed that the delocalization indices increase in the same manner as the  ${}^5J_{\text{H,H}}$  values, in agreement with the dominant role of the Fermi contact term and the delocalization index (Figure 3b) and is very similar to the one involving all the contributions to the coupling constant (Figure 3a).

Even though, the Fermi-hole density—involved in the definition of the delocalization index—is not a monotonous function of the distance between particles,<sup>25</sup> in the case of long-range couplings, the values of  $\delta(\text{H,H}')$  decrease quickly with the number of bonds that separate the nuclei involved. For example, for 9-bromoanthracene, the delocalization index is  $\delta(\text{H}_1,\text{H}_3) = 149 \times 10^{-5}$  and  $\delta(\text{H}_1,\text{H}_4) = 34 \times 10^{-5}$ , corresponding to atoms separated by four and five bonds, respectively. However, both the experimental coupling constants and their Fermi contact contribution decrease in parallel form and do not depend on the number of bonds involved.

${}^4J_{\text{H,H}'}$  values do not behave as the previous ones. Delocalization indices  $\delta(\text{H}_1,\text{H}_3)$  and  $\delta(\text{H}_2,\text{H}_4)$  and Fermi contact term behave linearly with  ${}^4J_{\text{H}_1\text{H}_3}$  and  ${}^4J_{\text{H}_2\text{H}_4}$  values. The  ${}^4J_{\text{H}_4\text{H}_{10}}$  deserves a separate analysis. All calculated Fermi contact terms for this coupling are negative. The corresponding delocalization indices are the largest for all couplings, e.g.,  $\sim 900 \times 10^{-5}$ .



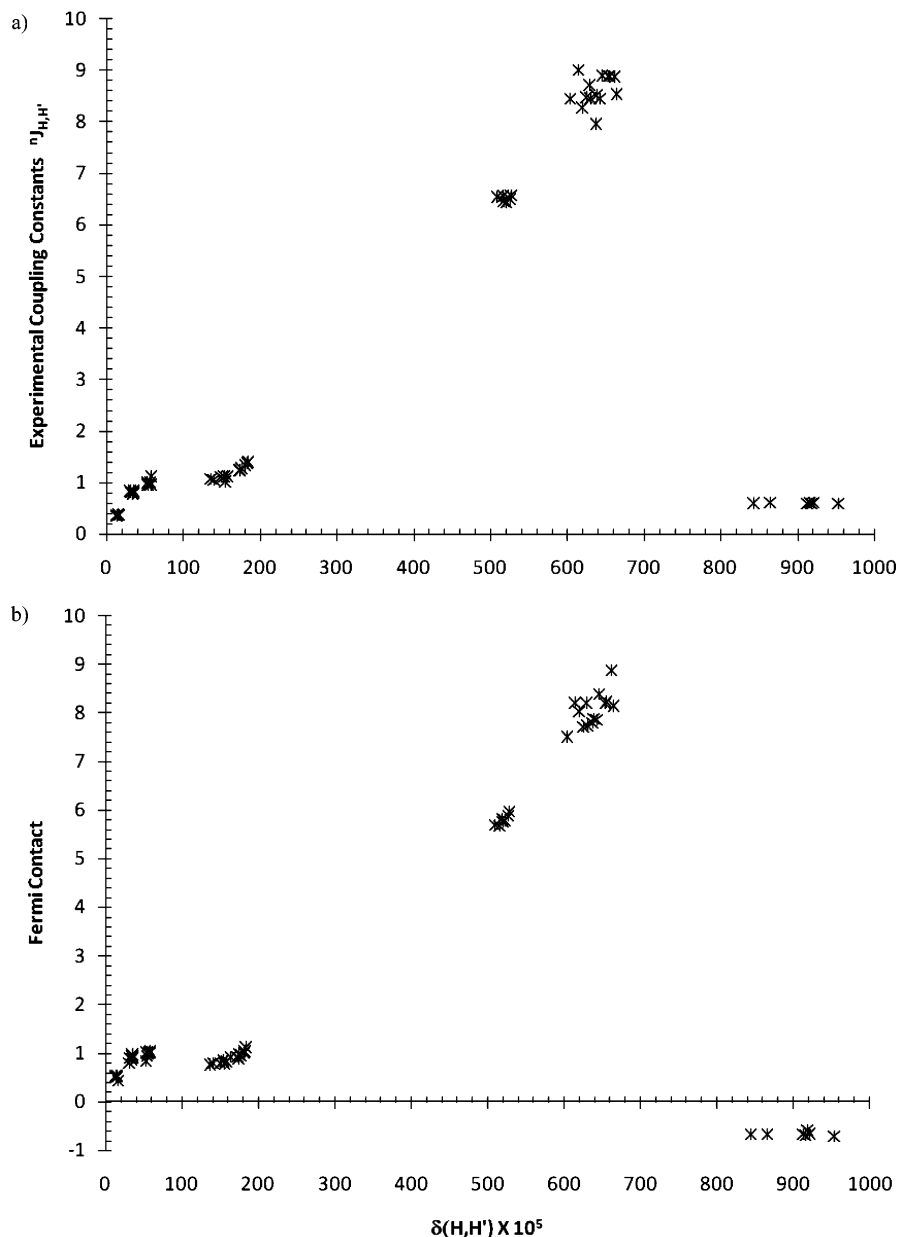


**Figure 3.** Behavior of the delocalization indices using the B3LYP/6-311+G(2d,p) level of theory vs (a) experimental coupling constant and (b) Fermi contact term. Coupling constants are grouped according with the number of bonds. The Fermi contact term and delocalization indices have a linear correlation, except for those coming from the  ${}^4J_{H4,H10}$ , which have a negative sign. In addition, in these couplings the delocalization indices have the highest values of all the indexes studied.

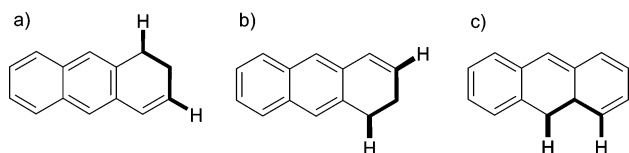


**Figure 4.** Geometrical arrangement for  ${}^4J_{H,H'}$ . (a)  ${}^4J_{H1,H3}$  and (b)  ${}^4J_{H3,H4}$  show the M or W conformation. (c)  ${}^4J_{H4,H10}$  showing a gable roof conformation.

These results could be characteristic of the different geometric arrangements that  ${}^4J_{H,H'}$  values have; see Figure 4.  ${}^4J_{H1,H3}$  and  ${}^4J_{H2,H4}$  present a known W or M shape (Figure 4a,b);  ${}^4J_{H4,H10}$  shows what we have called a “gable roof” arrangement formed by five nuclei involved in the coupling (Figure 4c). It seems that the geometry between the nucleus to four-bond H4 and H10 is an extension of the geminal arrangement, which causes a similarity in coupling signs and negative Fermi contact terms.

## Conclusion

Accurate experimental determinations of coupling constants of 9-anthracene derivatives allowed us to exhaustively analyze theoretical predictions for vicinal and long-range scalar coupling constants. Experimental reported data were obtained with an error of  $\pm 0.04$  Hz. Our comparison shows that one specific basis set cannot predict all coupling constants accurately. The B3LYP/6-31G\*\* level of theory can be used for three-bond coupling constants.  ${}^3J_{H1,H2}$  is the only coupling constants that shows important changes due to modification by the substituent. The B3LYP/6-311+G(2d,p) calculations better reproduce the  ${}^5J_{H,H'}$ . For  ${}^4J_{H,H'}$ , surprisingly, STO-3G basis set predicts the absolute value; the PSO terms undergo the largest changes for these couplings. We consider that the B3LYP/6-311+G(2d,p) level of theory reasonably reproduces all coupling constants, though. Vicinal coupling constants can be estimated by their contact Fermi term only. However, all other couplings depend on all

terms. DFT theoretical models can predict, in several cases, the exact value of spin–spin coupling constants, allowing us to extract the physical meaning of these parameters.

Delocalization indices for 9-anthracene derivatives linearly correlate with vicinal and long-range coupling constants. However, the analysis of these correlations should be separated by the coupling types.  ${}^4J_{H4,H10}$  values do not correlate linearly with the other delocalization indices. It can be inferred that the geometry of the nuclei involved in the coupling modifies its value. Geometric parameters may be playing a major role on the Fermi contact term and delocalization indices. The four-bond gable roof arrangement generates the largest delocalization indices and negative Fermi contact terms.

9-Anthracene derivatives were used as a model where degrees of freedom are restricted by the planarity of the molecules. Electron delocalization was shown to play a major role in the trends observed for H,H' coupling constants ranging from vicinal to those involving M or W arrangements of four and five bonds, due to the dominant role of the Fermi contact term. It is remarkable that the delocalization index, defined in terms of the pair-density, correlates well with such long couplings. Accurate determination of spin–spin coupling constants constitutes a real challenge for theoretical analysis and can be used as a test for new theoretical models.

## Experimental Methods

**Determination of Coupling Constants.** All compounds are commercially available (Aldrich) and were used without further purification. All experiments were carried out in  $CDCl_3$ . The  ${}^1H$  NMR spectra were obtained on a Bruker Advance DMX500 spectrometer operating at 500 MHz at room temperature. Chemical shifts were referenced to internal TMS. Shimming was performed until the TMS signal showed a resolution better than 0.4 Hz. Acquisition time for all samples was 10 s. Spectra were processed using only a baseline correction and no further apodization. All measurements were obtained using the modified  $J$  doubling method<sup>2,3</sup> in both signals involved in the coupling. The biggest coupling constants were determined and deconvolved for each multiplet. Then, this process was repeated to obtain the next bigger coupling, until all were extracted. For extreme cases, where several successive deconvolution processes do not generate well-defined line shapes, data were confirmed by removing from the original experimental signals a set of nonsuccessive coupling constants; when this procedure generates a well-behaved line shape, then it confirms a correct determination. We used 128 delta functions for vicinal coupling constants and 64 for long-range. Coupling constant signs were obtained by the double resonance method described by Freeman.<sup>32</sup> We referenced all signs on the basis of vicinal couplings as positives. All determination signs are clear due to the dispersion signals. However, all  ${}^4J_{H4,H10}$  signs were not measured because the coupling is immerse in the multiplet.

## Theoretical Calculations

Coupling constants were calculated within the DFT approach with the GIAO method including the four contributing terms and the B3LYP density exchange–correlation potential with *Gaussian 03*.<sup>34</sup> The B3LYP density functional provides accurate coupling constant values in many systems.<sup>35</sup> Several structures were fully optimized using the STO-3G, 3-21G, 6-31G, 6-31G\*, 6-31+G(d), 6-31G\*\*, and 6-311+G(2d,p) basis sets. Our discussion focused only on the results with the STO, 6-31G\*\*, and 6-311+G(2d,p) basis sets, because 3-21G, 6-31G, 6-31G\*, and 6-31+G(d) systematically underestimate coupling constants

(see the Supporting Information). The overlap integrals over the topological atoms in the molecules were computed with the program *AIMALL97*.<sup>36</sup> Delocalization indices were obtained according to eq 1.

**Acknowledgment.** This work was partially supported by CONACYT project 38616 (F.R.P.) ESM wants to thank CONACYT for the scholarship. We are in debt with Marco Antonio Vera for technical support.

**Supporting Information Available:** Two tables for all  ${}^nJ_{H,H}$  obtained by different levels of theory. This material is available free of charge via the Internet at <http://pubs.acs.org>.

## References and Notes

- (1) Eberstadt, M.; Gemmecker, G.; Mierke, D.; Kessler, H. *Angew. Chem. Int.* **1995**, *34*, 1671.
- (2) Garza-García, A.; Ponzanelli-Velazquez, G.; del Río-Portilla, F. J. *Magn. Reson.* **2001**, *148*, 214.
- (3) del Río-Portilla, F.; Sánchez-Mendoza, E.; Constantino-Castillo, V.; Del Río Portilla, J. A. *Arkivoc* **2003**, *2003*, 203.
- (4) Cobas, J. C.; Constantino-Castillo, V. M.; Martín-Pastor, M.; del Río-Portilla, F. *Magn. Reson. Chem.* **2005**, *43*, 843.
- (5) Ramsey, N. F.; Purcell, E. M. *Phys. Rev.* **1952**, *85*, 143.
- (6) Ramsey, N. F. *Phys. Rev.* **1953**, *91*, 303.
- (7) Malkin, V. G.; Malkina, O. L.; Salahub, D. R. *Chem. Phys. Lett.* **1994**, *221*, 91.
- (8) Malkina, O. L.; Salahub, D. R.; Malkin, V. G. *J. Chem. Phys.* **1996**, *105*, 8793.
- (9) Helgaker, T.; Jaszuski, M.; Ruud, K.; Górska, A. *Theor. Chem Acc.* **1998**, *99*, 175.
- (10) Helgaker, T.; Watson, M.; Handy, N. C. *J. Chem. Phys.* **2000**, *113*, 9402.
- (11) Autschbach, J.; Ziegler, T. *J. Chem. Phys.* **2000**, *113*, 9410.
- (12) Sychrovsky, V.; Gräfenstein, J.; Cremer, D. *J. Chem. Phys.* **2000**, *113*, 3530.
- (13) Karplus, M. *J. Chem. Phys.* **1959**, *30*, 11.
- (14) Karplus, M. *J. Phys. Chem.* **1960**, *64*, 1793.
- (15) Karplus, M. *J. Am. Chem. Soc.* **1963**, *85*, 2870.
- (16) Contreras, R. H.; Peralta, J. E. *Prog. NMR Spectrosc.* **2000**, *37*, 321.
- (17) Tomas, W. A. *Prog. NMR Spectrosc.* **1997**, *30*, 183.
- (18) Barfield, M.; Dean, A. M.; Fallick, C. J.; Spear, R. J.; Sternhell, S.; Westerman, P. W. *J. Am. Chem. Soc.* **1975**, *97*, 1482.
- (19) Constantino, M.; Lacerda, V.; Tasic, L. *J. Mol. Struct.* **2001**, *597*, 129.
- (20) Barfield, M.; Spear, R. J.; Sternhell, S. *J. Am. Chem. Soc.* **1971**, *93*, 5322.
- (21) Facelli, J. C.; Contreras, R. H.; Kowalewski, D. G.; Kowalewski, V. J.; Piegai, R. N. *J. Mol. Struct. Theochem.* **1983**, *94*, 163.
- (22) Bader, R. F. W. *A Quantum Theory*; Oxford University Press: Oxford U.K., 1990.
- (23) Matta, C. F.; Hernández-Trujillo, J. *J. Phys. Chem. A* **2003**, *107*, 7496.
- (24) Hernández-Trujillo, J.; Cortés-Guzmán, F.; Cuevas, G. Applications of the Quantum Theory of Atoms in Molecules in Organic Chemistry—Charge Distribution, Conformational Analysis and Molecular Interactions. In *The Quantum Theory of Atoms in Molecules*; Matta, C. F., Boyd, R. J., Eds.; Wiley-VHC: Weinheim, 2007.
- (25) Matta, C. F.; Hernández-Trujillo, J.; Bader, R. F. W. *J. Phys. Chem. A* **2002**, *106*, 7369.
- (26) Bader, R. F. W.; Streitwieser, A.; Neuhaus, A.; Laiding, K. E.; Speers, P. *J. Am. Chem. Soc.* **1996**, *118*, 4959.
- (27) Bartle, K. D.; Jones, D. W.; Matthews, R. S. *Tetrahedron* **1969**, *23*, 2701.
- (28) Schuster, I. I. *J. Org. Chem.* **1981**, *46*, 5110.
- (29) Ligabue, A.; Pincelli, U.; Lazzaretti, P.; Zanasi, R. *J. Am. Chem. Soc.* **1999**, *121*, 5513.
- (30) Lazlo, P. Solvent Effects and Nuclear Magnetic Resonance. In *Progress in NMR Spectroscopy*; Emesley, J. W., Feeney, J., Sutcliffe, L. H., Eds.; Elsevier: New York, 1967; Vol. 3, pp 348.
- (31) Katritzky, A. R.; Akhmedov, N. G.; Güven, A.; Scriven, E. F. V.; Majumder, S.; Akhmedova, R. G.; Hall, D. *J. Mol. Struct.* **2006**, *783*, 191.
- (32) Freeman, R.; Whiffen, D. H. *Mol. Phys.* **1961**, *4*, 321.
- (33) Günther, H. Z. *Naturforschung, B* **1969**, *24*, 680.
- (34) Frisch, M. J.; Trucks, G. W.; Schlegel, H. B.; Scuseria, G. E.; Robb, M. A.; Cheeseman, J. R.; Montgomery, J. A., Jr.; Vreven, T.; Kudin, K. N.; Burant, J. C.; Millam, J. M.; Iyengar, S. S.; Tomasi, J.; Barone, V.; Mennucci, B.; Cossi, M.; Scalmani, G.; Rega, N.; Petersson, G. A.;

Nakatsuji, H.; Hada, M.; Ehara, M.; Toyota, K.; Fukuda, R.; Hasegawa, J.; Ishida, M.; Nakajima, T.; Honda, Y.; Kitao, O.; Nakai, H.; Klene, M.; Li, X.; Knox, J. E.; Hratchian, H. P.; Cross, J. B.; Bakken, V.; Adamo, C.; Jaramillo, J.; Gomperts, R.; Stratmann, R. E.; Yazyev, O.; Austin, A. J.; Cammi, R.; Pomelli, C.; Ochterski, J. W.; Ayala, P. Y.; Morokuma, K.; Voth, G. A.; Salvador, P.; Dannenberg, J. J.; Zakrzewski, V. G.; Dapprich, S.; Daniels, A. D.; Strain, M. C.; Farkas, O.; Malick, D. K.; Rabuck, A. D.; Raghavachari, K.; Foresman, J. B.; Ortiz, J. V.; Cui, Q.; Baboul, A. G.; Clifford, S.; Cioslowski, J.; Stefanov, B. B.; Liu, G.; Liashenko, A.; Piskorz, P.; Komaromi, I.; Martin, R. L.; Fox, D. J.; Keith, T.; Al-Laham,

M. A.; Peng, C. Y.; Nanayakkara, A.; Challacombe, M.; Gill, P. M. W.; Johnson, B.; Chen, W.; Wong, M. W.; Gonzalez, C.; Pople, J. A. *Gaussian 03*, Revision C.02; Gaussian, Inc., Wallingford, CT, 2004.

(35) Helgaker, R.; Pecul, M. Spin-Spin Coupling Constants with HF and DFT Methods. In *Calculation of NMR and EPR Parameters*; Kaupp, M., Bühl, M., Malkin, V. G., Eds.; Wiley-VCH: Weinheim, 2004.

(36) AIMALL97 Package (D1) for Windows (aim@tkgristmill.com).

(37) Arciniegas, A.; Pérez-Castorena, A.; Cuevas, G.; del Río-Portilla, F.; Romo de Vivar, A. *Magn. Reson. Chem.* **2006**, *44*, 30.